ARABIDOPSIS PEX19 IS A DIMERIC PROTEIN THAT BINDS THE PEROXIN PEX10

Dawn A. Hadden*[1], Belinda A. Phillipson[2], Laura-Anne Brown, Mahmoud El-Shami[3], Imogen A. Sparkes[4] and Alison Baker.

Centre for Plant Sciences, University of Leeds, Leeds, LS2 9JT

Running title: *Arabidopsis* PEX19

Present address: [1]Biosciences, Sheffield Hallam University, Sheffield, UK. [2]Central Science Laboratory, Sand Hutton, York, UK. [3]Al-Azhar, University, Nasser City Egypt. [4]School of Biological and Molecular Sciences, Oxford Brookes University, Gypsy Lane, Oxford, UK. *Address correspondence to; Dawn A. Hadden, Biosciences, Sheffield Hallam University, Sheffield, S1 1WB, UK. Tel +44 (0)114 225 3038, e-mail d.hadden@shu.ac.uk.

PEX19 is a predominantly cytosolic, farnesylated protein of mammalian and yeast cells that binds multiple peroxisome membrane proteins and is required for their correct targeting/insertion to the peroxisome membrane. Here we provide functional characterisation of *Arabidopsis* PEX19 (AtPEX19), which is encoded by two genes that are expressed in all tissues and at all developmental stages of the plant. Like its yeast and mammalian counterparts AtPEX19 is predominantly cytosolic and binds the peroxisomal membrane protein AtPEX10. Farnesylation of AtPEX19 is not required for PEX10 binding. We further provide evidence that AtPEX19 is a dimer and that the dimer preferentially forms complexes with other proteins *in vivo*. Based on our data and that of others we propose a model for the recognition of peroxisomal membrane proteins by PEX19 and their PEX3 dependent integration into the peroxisome membrane.

Peroxisomes are single-membrane bound metabolic organelles, found in virtually all eukaryotes. There are two conserved functions of peroxisomes found amongst evolutionary diverse organisms, namely β-oxidation of fatty acids and hydrogen peroxide metabolism. Other specialised roles depend on the organism and cell type.

Plant peroxisomes are involved in a range of important functions such as the mobilisation of storage reserves in germinating seedlings via β-oxidation and the glyoxylate cycle [1], the salvage of carbon through photorespiration [2] and defence against oxidative stresses [3]. Plant peroxisomes are also implicated in the generation of a variety of significant hormones and other signalling molecules, including indole acetic acid [4], jasmonate [5, 6], nitric oxide and several reactive oxygen species [3]. It has also emerged that plant peroxisomes are involved in light regulated gene expression [7], embryogenesis [8, 9] and the breaking of seed dormancy [10].

Although peroxisome function varies between species, the biogenesis of peroxisomes relies on a common class of conserved genes, referred to as *PEX* genes, which encode proteins termed peroxins. To date, over thirty peroxins have been identified. They are involved in peroxisomal matrix protein import, membrane biogenesis and organelle proliferation, although their exact mechanistic functions are still only partially understood. The mechanisms used for importing peroxisomal membrane proteins (PMPs) are distinct from those that translocate proteins into the peroxisomal matrix. Only three peroxins potentially play a role in PMP targeting: PEX3 [11, 12], PEX16 [13, 14]; and PEX19 [15-18]. Recent observations in *Saccharomyces cerevisiae* have shown that an interaction between Pex3 and Pex19 is necessary for peroxisome biogenesis at the endoplasmic reticulum [19]. In cells deficient in any of these peroxins, PMPs are either degraded or mistargeted to other subcellular locations [11, 20, 21].

PEX19 has been identified as a candidate for both a chaperone [22] and a receptor [21] for PMPs. Many *pex19* mutants lack any detectable peroxisome membranes, or have low levels of PMPs which are mislocalised to the cytosol or mitochondria [11, 21]. However in *pex19* mutants

of *Y. lipolytica, H. polymorpha* and *P.pastoris,* small vesicular structures similar in density to wild type peroxisomes and containing some matrix proteins, were found [17, 23, 24]. There is controversy regarding whether PEX19 preferentially binds newly synthesised [25] or existing [22] PMPs, or whether it may even play a role in the assembly of protein complexes in the peroxisome membrane [26]. There is also disagreement as to whether PEX19 binds a region that contains peroxisomal targeting information (mPTS) and therefore functions as a PMP receptor [21, 25], or if PEX19 binding and PMP targeting are separable events [26, 27]. Recently, the Pex19p binding sites on several *Saccharomyces* PMPs have been experimentally determined and shown to be essential for correct targeting, providing strong evidence for a receptor function for Pex19p [28]. Targeting of PMPs also requires at least one transmembrane domain (TMD) in addition to the PEX19 binding site, in order to bring about correct localisation to peroxisomes [28]. Thus an mPTS has two functionally distinct domains, a PEX19 binding site and a TMD.

The cellular distribution of PEX19 (predominantly cytosolic with a small amount associated with peroxisomes) is consistent with a function in shuttling PMPs from the cytosol to the peroxisome membrane. The integral peroxisome membrane protein PEX3 has been shown to act as a receptor for PEX19 [29]. Membrane association of PEX19 has been suggested to be through farnesylation of the C-terminus at a conserved prenylation motif (CaaX box). However, there are conflicting reports as to whether farnesylation of PEX19 is important for function [16, 17, 21, 27]. PEX19 has a broad specificity, binding to many PMPs and domain mapping of the protein [30-32] has led to the suggestion that it may bind PMPs in multiple places for multiple functions [30].

We have characterised a homologue of PEX19 from *Arabidopsis thaliana*. We show that AtPEX19 is predominately cytosolic with the membrane associated fraction partly peroxisomal. *In vitro* translated and recombinant AtPEX19 binds to the PMP, AtPEX10, and the recombinant protein has a two-domain structure similar to the human protein, thus suggesting that structure and function is conserved between plants and humans. We also provide evidence that AtPEX19 is a dimer *in vitro* and that the dimeric form is preferentially cross-linked to other proteins *in vivo*: a novel feature not yet demonstrated in yeast or mammalian PEX19.

EXPERIMENTAL PROCEDURES

Constructs for expression of recombinant PEX19 and GST-Pex10$_{267\text{-}381}$ - Molecular biology methods were carried out according to Sambrook & Russell [33]. EST clone ATTS4952 encoding AtPEX19-1 was obtained from Dr Thierry Desprez, INRA, Versailles, France. The *PEX19-1* (At3g03490) reading frame was amplified by PCR using primers 5'-GCGGAATTCGGCGAACAGTCACACCGAT-3' and
5'-CGCGCCTCGAGTCACATGATACAGCAATT-3' that introduced an *Eco*RI site adjacent to the second amino acid (Ala) and an *Xho*I site down stream of the termination codon, and recloned into pET28(b) (Novagen) cut with the same restriction enzymes. The encoded protein is referred to as His_6T7PEX19 as it contains both the His and T7 tags N-terminal to PEX19 and has a theoretical pI of 5.00 and Mw of 31,842. A similar construct where PEX19 was cloned into the *Nhe*I-*Sac*I sites of pET28(a) was obtained from Dr Susanna Cristobal, Uppsala University Sweden. This encodes a protein we refer to as His_6PEX19 as it lacks the T7 tag and has a theoretical pI of 5.00 and Mw of 30,482. When expressed in *E. coli* His_6T7PEX19 is insoluble but can be solubilised and refolded whereas His_6PEX19 is expressed in a soluble form. His_6T7PEX19 was used for antibody production and the co-immunoprecipitation experiment. His_6PEX19 was used in all other experiments.

The carboxyl terminal region of At*PEX10* (At2g26350) cDNA was amplified using Gateway primers (forward strand 5'-GGGGACAAGTTTGTACAAAAAAGCAGGCT TCATGCGTCGGAGTAATTTGTCA-3' and reverse strand 3'-GGGGACCACTTTGTACAAGAAAGCTGGGT TCTAAAAATCAGAATGATACAA-5') with PfuTurbo proofreading DNA polymerase (Stratagene). The PCR product was inserted in the Gateway donor vector pDONR201 (Invitrogen) via the Gateway BP reaction and then transferred into

pDEST15 (Invitrogen) via the Gateway LR reaction

Bacterial culture for protein expression- His_6PEX19 and GST-$Pex10_{267-381}$ were expressed in *E. coli* BL21 (DE3) pLysS cells (Novagen) and His_6T7PEX19 in BL21 (DE3) Codon Plus RIL cells (Invitrogen), as described (Novagen pET hand book 10th edition (www.novagen.com). The majority of the His_6T7PEX19 protein was insoluble, and so the inclusion bodies were solubilised in 20 mM Na phosphate buffer pH 7.5, 10 mM imidazole, 0.5M NaCl, 8M urea (50 µl/ml culture) and solubilised protein was purified by passage over a Ni^{2+} column (GE Healthcare) according to the manufacturer's instructions. The purified protein was dialysed overnight at 4ºC against 20 mM Na phosphate buffer pH 7.5. The purified protein was used to raise polyclonal antibodies in rabbits (Scottish Antibody Production Unit, Carluke, Scotland). His_6PEX19 was soluble and was purified on a 5ml Hi-Trap nickel affinity column (GE Healthcare) according to the manufacturers instructions. For molecular weight estimation using gel filtration chromatography, 1.5 ml of purified His_6PEX19 (10 mg/ml) was applied in 50 mM NaCl, 20 mM Tris pH 8.0, to a Superdex 75 26/60 column (GE Healthcare), pre-equilibrated in the same buffer. For the production of soluble GST-$Pex10_{267-381}$, when absorbance of the culture at 600 nm reached 0.4, it was heat-shocked at 45ºC for 20 minutes then cooled rapidly to 18 ºC. IPTG was added to 0.5 mM and the culture incubated at 18ºC, 200 rpm for a further 4 hours.

Isolation of His_6PEX19-GST-$Pex10_{267-381}$ complex- Cell pellets from 400 ml cultures of BL21(DE3)pLysS expressing His_6PEX19 and BL21(DE3)pLysS expressing GST-$Pex10_{267-381}$ were individually resuspended in 10 ml PBS, 1 mM DTT containing 5 mg lysozyme and a COMPLETE™ protease inhibitor tablet (Roche). The suspensions were incubated for 20 minutes on ice then sonicated 6 times for 30 seconds on/30 seconds off, before centrifugation at 20,000g for 30 minutes at 5ºC. The supernatants were applied to a 1 ml glutathione agarose column (Sigma) either singly or as a mixture. The column was washed with 20 ml PBS and bound proteins eluted stepwise with PBS containing 10 mM reduced glutathione in 2 ml fractions. The fractions were examined by SDS-PAGE and Western blot. PEX19 was visualised using antisera raised to His_6T7PEX19 at a 1:10,000 dilution followed by goat anti-rabbit IgG-horse radish peroxidase (Sigma, 1:10,000 dilution) with enhanced chemiluminescent detection.

Cross-linking Arabidopsis cells in vivo with formaldehyde- Arabidosis cells suspension [34] were grown in 100 ml MS medium (4.43g/L, sucrose 30g/L, NAA 0.5mg/L, and Kinetin 0.05mg/L, pH, 5.8) at 24ºC under dim light with a 16-hour photoperiod in a rotary shaker at 110 rpm. The cells were split every seven days at a 1:10 dilution into the same media. A 100 ml culture was centrifuged at 1000 rpm, the cell pellet was resuspended in PBS containing 1% formaldehyde and incubated at room temperature for 1 hour. To quench the reaction glycine was added to a final concentration of 300 mM in PBS and incubated for a further 30 minutes. The cells were centrifuged at 1000 rpm and washed by re-suspension in PBS before further centrifugation and flash freezing in liquid nitrogen. 5g of frozen cells were ground to powder under liquid nitrogen and added to 15 ml 50 mM Tris, pH 7.5, 1% SDS containing 1 µM E-64 (Sigma), 1 COMPLETE™ protease inhibitor tablet (Roche) and 100 µl Plant Protease inhibitor cocktail (Sigma). The suspension was agitated for 30 minutes at 4ºC before centrifugation at 10,000g for 20 minutes at 4ºC. The supernatant was removed and heated in SDS-PAGE sample buffer at 65ºC for 3 minutes before immediate analysis by Western blotting as previously described

Isolation of membrane and organelle fractions from cell cultures- Sucrose density gradient and assay of fractions were performed as described [35]. For total membrane isolation, cells (2g) were collected by filtration onto nitro-cellulose filters. They were ground to a fine powder in presence of liquid nitrogen and resuspended in 10 ml of homogenisation buffer, (25 mM Hepes / KOH. pH 7.5, 300 mM Sucrose, 1mM DTT, 2 mM o-phenanthroline, 1.4 µg/L Pepstatin, 0.5µg/L Leupeptin, 2µg/L aprotinin, and 1µg/L Trans-epoxysucinyl-L-Leucylamido- (4-guanido)-butane). The homogenate was filtered through one layer of Miracloth (Calbiochem) followed by two layers of gauze. The filtered homogenate was centrifuged at 5,000 g for 15 minutes at 4ºC. The 5,000g supernatant was centrifuged at 100,000 g for 1 hour at 4ºC to separate total membranes

(pellet) from the cytosol (supernatant). Western blotting was carried out as previously described. Anti-His_6T7PEX19 serum was used at 1:5,000-1:10,000 dilution. Anti-thiolase serum was used at 1:50,000 dilution.

Co-immunoprecipitation- His_6T7PEX19 and PEX10 (in pGEM-T easy) were transcribed and translated in a coupled wheatgerm lysate system (TNT) in the presence of [^{35}S] L-methionine according to the manufacturers (Promega) protocol. After 90 minutes at 30ºC, equal volumes (25µl) of His_6T7PEX19 and PEX10 translation reactions were mixed and incubated for a further 90 minutes at 30ºC then immunoprecipitated with either non immune antiserum or anti poly-His antiserum. Siliconized tubes were used to avoid non-specific binding of radio-labelled proteins. Twenty two microlitres of each reaction were diluted into 0.55 ml IP buffer (50 mM Tris HCl pH 7.5, 150 mM NaCl, 5mM EDTA, 1% v/v Triton-X-100, plus 1 COMPLETE™ protease inhibitor cocktail tablet (Roche) per 50 ml) with 50 µl of protein A beads (prewashed in IP buffer) and incubated with gentle shaking at 4ºC for 1 hour. The beads were removed by centrifugation and the supernatants removed to a clean tube and anti-serum (1:50 dilution) added and incubated 60 minutes 4ºC with gentle agitation. A further 50 µl protein A beads were added and incubated as before. Immunoprecipitated proteins were recovered by centrifugation and the beads extensively washed in IP buffer. The final washed pellet was resuspended in SDS-PAGE sample buffer and solubilised at 37°C for 60 minutes before SDS-PAGE and detection by phosphoimaging.

RESULTS

Arabidopsis thaliana has two PEX19-like genes- The *Arabidopsis thaliana* genome contains two reading frames At5g17550 and At3g03490 with significant homology to human Pex19p (28.2% amino acid identity) and *Saccharomyces cerevisiae* Pex19p (24.5% amino acid identity) (Fig. 1). An EST (ATTS4952 GI:773437) corresponding to At3g03490, which we have designated At*PEX19-1* was fully sequenced (accession number AJ564199). At*PEX19-1* and At*PEX19-2* are 82% identical to one another at the nucleotide level and 79% identical at the amino acid level. All four proteins share conserved CAAX box motifs at the carboxyl terminus. In addition there are two regions that are particularly well conserved. The first is a block of 13 alternating acidic and hydrophobic residues near the amino terminus that are predicted to form a perfect acidic amphipathic helix (http://www.site.uottawa.ca/~turcotte/resources/HelixWheel/) and a second region in the C-terminal half of the protein that also shares alternating polar and hydrophobic residues and a predicted helical structure (Fig. 1). Using the secondary structure prediction program GOR4, *Arabidopsis* PEX19 is estimated to be predominantly α-helical (58%) with a substantial proportion of random coil (36.7%) [36]. Our circular dichroism (CD) analysis of recombinant His_6PEX19 indicated 25-50% helix, 9-27% strand, 14-24% turn and 27-30% unordered structures depending on the method and reference set to fit the data (data not shown).

To determine whether both genes were expressed, gene specific primers were designed and used in a reverse-transcription PCR reaction with total RNA derived from different *Arabidopsis* tissues. Both genes are expressed in essentially all tissues including seedlings, roots, young and senescent leaves, flowers, siliques and stems (data not shown). To obtain a more detailed expression profile, public microarray data derived from the Affymetrix 22k chip was analysed using the GENEVESTIGATOR web site (https://www.genevestigator.ethz.ch/[37]). At*PEX19-2* (At5g17550) is not present on the 22k chip so only results for At*PEX19-1* are presented (Fig. 2). *PEX19-1* is most highly expressed in young seedlings, age 1-5.9 days, corresponding to stage 0.1-0.70 [38]. Levels then remain fairly constant throughout development before increasing as the plants produce seeds (stage 8). Consistent with this, the highest level of expression is in stamens and seed. High levels are also seen in cell suspension cultures (Fig. 3A).

Arabidopsis PEX19 is a predominantly cytosolic protein- Antibodies were raised against recombinant His_6T7PEX19, which detected a protein of about 30 kDa in 2 day *Arabidopsis* seedlings (Fig. 3A, lane 3 left panel). This protein was absent when the antibodies were preincubated with the recombinant His_6T7PEX19 (Fig. 3A right panel). The antibody readily detected 10 and even 1 ng of recombinant His_6T7PEX19 which has a

molecular weight of 31,842 (Fig. 3A left panel lanes 1 and 2). Due to the high degree of similarity between PEX19-1 and PEX19-2 we assume the antibody detects both isoforms in plant samples and therefore refer to the cross-reacting band as AtPEX19. To determine the localisation of AtPEX19 in *Arabidopsis* cells we used a suspension culture cell line. These suspension culture cells have abundant peroxisomes as shown by electron microscopy (data not shown). Suspension culture cells were fractionated into a total membrane and soluble fraction and probed with anti-PEX19 antibodies. PEX19 was recovered predominantly in the cytosol (Fig. 3B lane C), with only a small proportion associated with the membrane fraction. (Fig. 3B lane M). Sucrose density gradient centrifugation was used to prepare organelle fractions from tissue culture cells. The position of peroxisomes was determined by immunoblotting with the marker protein thiolase (Fig. 3C top panel). This shows that intact peroxisomes are found predominantly in fractions 4-7 with a substantial amount of thiolase found at the top of the gradient, which represents protein that has been released from damaged organelles. A duplicate blot was probed with anti PEX19 antibodies, where native PEX19 (Fig. 3C lower panel, arrow) was mainly found at the top of the gradient with a minute amount co-sedimenting with peroxisomes, although there is a prominent doublet that is enriched in the peroxisomal fractions that migrates with approximately twice the expected molecular weight of PEX19 (Fig. 3C lower panel). Thus it is thought that AtPEX19 is predominantly cytosolic.

Arabidopsis PEX19 forms a dimer- His_6PEX19 was over expressed as a soluble protein in *E. coli*. The recombinant protein was purified to near homogenetiy using nickel affinity chromatography, with a molecular mass determined by matrix assisted laser desorption/ionisation mass spectrometry to be 30,479 (not shown), which was consistent with the calculated mass. However, when analysed by gel filtration chromatography, the purified protein was shown to elute with a retention volume corresponding to a protein of approximately 60 kDa (Fig. 4 A). This was determined by comparison to molecular weight calibration proteins. The data suggests that PEX19 forms a dimer which is extremely stable, since little monomeric protein was observed. When analysed by SDS-PAGE, rHis_6PEX19 migrated with an apparent molecular mass of slightly greater than 30 kDa consistent with denatured, monomeric polypeptide chains (Fig. 4 B).

In vitro translated and recombinant PEX19 binds PEX10- In other organisms Pex19p binds to a range of PMPs including Pex10p [17]. The ability of AtPEX19 to bind to AtPEX10 was tested via co-immunoprecipitation (Fig. 5). *In vitro* translations of the individual full length proteins were mixed, incubated together for 90 minutes at 30ºC then were subjected to immunoprecipitation under non-denaturing conditions with either non-immune serum (PI) or anti His antibody (H). PEX10 (open arrow) was clearly co-immunoprecipitated with His_6T7PEX19 (solid arrow) when anti-His tag antibody was used, but not when a non-immune serum was substituted for the primary antibody. PEX10 was equally efficiently precipitated with His_6T7PEX19 regardless of whether the proteins were translated separately and mixed or translated together (data not shown).

To establish whether the recombinant His_6PEX19 was able to bind PEX10, pull down experiments were performed. As full length AtPEX10 is unlikely to be soluble when expressed in *E. coli*, a fusion protein, GST–$PEX10_{267\text{-}381}$ was constructed. This corresponds to the region of PEX10, C-terminal to the predicted second transmembrane domain and includes the entire RING finger. Lysates from *E. coli* cells expressing GST-$PEX10_{267\text{-}381}$ or His_6PEX19 were applied singly, or as a mixture, to glutathione columns. The unbound material was collected and the column washed prior to elution with glutathione. The fractions were analysed by Western blotting using antibodies against His_6T7PEX19 and GST (Fig. 6). Where lysate containing His_6PEX19 was applied to the GST column on its own, (Fig. 6A middle panel) His_6PEX19 was recovered in the flow through (FT) and wash (W) fractions but not in the eluate fraction (E). However, when lysate containing PEX19 was mixed with lysate containing GST-$PEX10_{267\text{-}381}$, a portion of PEX19 was recovered in the glutathione eluate (Fig. 6 A, right most panel, lane E). When GST-$PEX10_{267\text{-}381}$ alone was applied to the column, as expected there was no PEX19 immunoreactivity in any fraction (Fig. 6A left most panel). A duplicate blot to that

shown in Fig. 6A was probed with anti-GST antibodies (Fig. 6B). GST-PEX10$_{267-381}$ binds to the column and is eluted with glutathione (Fig. 6B left and right most panels). When His$_6$PEX19 alone was applied to the column, no immunoreactivity was detected at the molecular weight corresponding to PEX19 (compare Fig. 6A) showing that the anti-GST antibodies do not cross react with PEX19 These results demonstrate that PEX19 is only retained on the glutathione column in the presence of GST-PEX10$_{267-381.}$ Therefore both *in vitro* translated and recombinant PEX19 bind to PEX10.

PEX19 binds to other proteins as a dimer in vivo- To examine the binding characteristics of *Arabidopsis* PEX19 *in vivo*, whole suspension cell culture cells were cross-linked using 1% formaldehyde and the cell lysate analysed by Western blotting (Fig. 7). Evidence that PEX19 binds to other proteins was apparent, since when subjected to the crosslinking procedure, the majority of the protein migrated down the gel with apparent masses of greater than 160 kDa, suggesting that binding complexes made with other proteins were rendered permanent by the procedure (Fig. 7A). Native PEX19 from the non-crosslinked cells migrated with molecular masses of approximately 30 and 60 kDa consistent with monomeric and dimeric protein. Interestingly, the band corresponding to the dimer was not observed in the crosslinked sample (Fig. 7A, left lane), indicating that the dimer may be preferentially involved in the formation of complexes with other proteins. To eliminate the possibility that the band thought to be a dimer in the non-crosslinked sample, is a result of non-specific binding by the antisera, samples were also analysed by Western blot using antisera incubated with 10 μg recombinant His$_6$PEX19 prior to immunodecoration of the blot (Fig. 7B). It must be noted that in Fig. 4B, recombinant His$_6$PEX19 migrated in SDS-PAGE only as an apparent monomer with mass of approximately 30 kDa, even though gel filtration chromatography indicated that the protein has a dimeric mass of 60 kDa. The fact that dimer was not seen on this SDS-PAGE, but was observed in the crosslinking study (Fig. 7 A), can be attributed to incomplete denaturing in SDS-PAGE sample buffer prior to loading the gel. In the crosslinking study, samples were heated to 65ºC in order to limit proteolytic action of native *Arabidopsis* enzymes, but were not boiled in order to minimise thermally induced aggregation of possible membrane protein-PEX19 complexes in the presence of SDS [39]. However, since samples collected from the gel filtration column were unlikely to contain membrane proteins, they were boiled in sample buffer for 3 minutes.

DISCUSSION

In this study we have characterised PEX19 from *Arabidopsis thaliana*. There are two genes encoding very similar PEX19 isoforms, both of which are expressed. Analysis of microarray data for *PEX19-1* shows expression in a range of cell types and developmental stages consistent with a requirement for maintenance of peroxisomes in a wide range of tissues. High levels of expression in cell suspension culture probably reflects the rapidly dividing nature of this undifferentiated tissue, whereas high levels of expression in seed is consistent with the requirement of peroxisomes for embryogenesis. Like its counterparts in mammals and yeasts, AtPEX19 is a predominantly cytosolic protein with only a small portion of the membrane-associated fraction migrating with peroxisomes, suggesting that the interaction with the peroxisome membrane is quite labile.

Conservation of structure between *Arabidopsis* and human PEX19 is apparent. Like human Pex19p [31], we also found that recombinant AtPEX19 is readily cleaved by thrombin and trypsin, resulting in a fragment of 20 kDa which is extremely stable to further digestion and which likely corresponds to the C-terminus (data not shown). Alignment of the sequences of the human and *Arabidopsis* PEX19s reveal that the lysine residue which was determined to be the trypsin cleavage site [31] is conserved in both AtPEX19-1 and AtPEX19-2. Secondary structure prediction using the program GOR4 [36] gives values of 58% alpha helix and 37% random coil for AtPEX19-1. CD analysis on purified His$_6$PEX19 also indicated a fairly high proportion (27-30%) of unordered structure. However, our CD data for the full length PEX19 protein indicates a much higher content of α-helix (25-50% depending on the method and reference set used to fit the data) than the 22% reported by for

human Pex19p [31], as well as significant amounts of strand (9-27%) and turn (14-24%).

On gel filtration we found that His_6PEX19 elutes with a retention volume corresponding to a molecular size of 60 kDa, although SDS-PAGE and MALDI-MS indicate only a single polypeptide chain, consistent with the calculated mass of His_6PEX19 and AtPEX19-1. The elution profile is very symmetric indicating a uniform population of molecules. Shibata *et al* [31] favoured the interpretation that the anomalous migration of human Pex19p on gel filtration was due to 'a certain distorted shape, caused by the disordered N-terminal region'. We think a more likely explanation is that PEX19 forms a stable dimer. Indeed on SDS-PAGE gels we often see a varying amount of a molecular species that reacts with anti-PEX19 antibody and is approximately twice the molecular weight of the monomeric PEX19. In Fig. 7 we show that this species is preferentially cross-linked *in vivo* and forms large heterogeneous complexes. As PEX19 is a relatively small protein it may function as a homo or hetero oligomer to keep large hydrophobic PMPs in solution. Interestingly Otzen *et al*. [24] showed by fluorescence correlation spectroscopy and native gels that *Hansenula polymorpha* Pex19p-GFP is detected in complexes of approximately 250 kDa. This is consistent with a homotetramer of 60 kDa HpPex19p-GFP molecules, although this interpretation is complicated by the fact that GFP itself has a tendency to dimerise at high concentrations [40].

Like its mammalian and yeast counterparts AtPEX19 binds the peroxisome membrane protein PEX10. The GST pull down experiments demonstrate that there is a binding site for PEX19 within the C terminus of AtPEX10. This is in line with previous results that showed that the region between amino acids 217 and 380 of *Pichia pastoris* Pex10p interacted with Pex19p in the yeast 2 hybrid system [17]. As the recombinant AtPEX19 is not farnesylated, the pull down experiments demonstrate that farnesylation is not required for PEX10 binding and that this interaction can take place post translationally. However this does not exclude the possibility that PEX19 can interact with nascent PMPs or that farnesylation could enhance or regulate PMP binding.

Recently Pex19p binding sites were identified and characterised in *S. cerevisiae* for Pex13p and ScPex11p and their importance for correct targeting *in vivo* demonstrated [28]. The essential features of these sites are that they are short 11mer linear peptides, most likely α-helical in nature and containing both hydrophobic and basic residues. How might these be recognised by PEX19? The alignment in Fig. 1 reveals two strikingly conserved regions between human, *S. cerevisiae* and *Arabidopsis* PEX19's. These two regions consist of alternating hydrophobic (shaded gray) and polar, often acidic, residues. For the *Arabidopsis* proteins both regions are predicted to lie within regions of alpha helix. Thus they would make attractive possibilities to bind a positively charged helical peptide. A similar molecular recognition event occurs between Tom20, a mitochondrial import receptor and the positively charged amphipathic α-helical mitochondrial-targeting signal. Tom20 binds the hydrophobic face of the peptide [41] and is also presumed to bind the charged face due to the presence of negatively charged domains within this protein [42]. Interestingly, when PEX19 is deleted or mutated several PMPs are mistargeted to mitochondria [21, 24], suggesting that in the absence of PEX19, the PEX19 binding motif could be recognised by the mitochondrial targeting machinery.

The integral peroxisome membrane protein PEX3 functions as a receptor for PEX19, where docking is thought to facilitates the insertion of the PMP cargo [29]. Our data together with recent publications from other groups allow us to propose a model for PEX19 function which provides an explanation for the two independent binding sites within PEX19 for PEX3 [30, 32]. The PEX3 binding site within the amino terminus of PEX19 has been mapped to the first 51 residues of human PEX19 [29] and first 42 residues of *Pichia* Pex19p [17]. This would encompass the highly conserved negatively charged amphipathic helix shown in Fig. 1, which is also a feature of the two *Arabidopsis* PEX19 proteins. This N-terminal region of PEX19 can interact with human PEX3 in the region 120-136 [29] (italics in Fig. 8A), and with yeast Pex3p in the region 130-160 predicted from the PEX19 binding site algorithm [28] (underlined in Fig. 8A), thereby providing the docking function for PEX19 at the peroxisome

membrane [29] (Fig. 8A). There is a second site in PEX19 which binds both PMPs and PEX3 [30] which overlaps the second conserved region in PEX19 (Fig. 1). This binding site must interact with a second PEX19 binding site in PEX3, which lies within the first 66 amino acids of human PEX3, because a naturally occurring splice variant of human PEX19 which lacks the first 87 amino acids of PEX19 can bind full length PEX3 but not the N terminal truncation [32]. Consistent with this Rottensteiner *et al* [28] predict a second Pex19p binding site within amino acids 25-50 of *Saccharomyces* Pex3p (underlined in Fig. 8A). This encompasses a region that contains a number of charged and hydrophobic residues. We propose that this N-terminal region of PEX3, which would lie close to the membrane surface (or possibly even on the membrane surface as amphipathic helix), would compete with the mPTS of the PMP cargo for binding to the second PEX19 binding site. This would release the mPTS and associated TMD in the vicinity of the membrane, where it could either insert spontaneously or integrate catalysed by PEX3 or some as yet unidentified factor. The function of PEX19 as a dimer would make sense, as many PMPs have two or more mPTS. Dimeric PEX19 could bind a PMP with two mPTS's and deliver these for release at the membrane surface allowing insertion of the two transmembrane domains as a helical hairpin. Dimeric PEX19 could in principle interact with one molecule of PEX3 sequentially, or two molecules of PEX3 simultaneously.

REFERENCES

1. Graham, I. A. and Eastmond, P. J. (2002) *Prog. Lipid Res.* **41**, 156-181
2. Reumann, S. (2002) in *Plant peroxisomes. Biochemistry, Cell biology and Biotechnological applications*, Baker, A. and Graham, I. A., Editors. Kluwer Academic Publishers, Dordrecht. p. 141-190.
3. Corpas, F. J., Barroso, J. B. and del Rio, L. A. (2001) *Trends Plant Sci.* **6**, 145-150
4. Zolman, B. K., Yoder, A. and Bartel, B. (2000) *Genetics* **156**, 1323-1337
5. Stintzi, A. and Browse, J. (2000) *Proc. Natl. Acad. Sci. U. S. A.* **97**, 10625-10630
6. Theodoulou, F. L., Job, K., Slocombe, S. P., Footitt, S., Holdsworth, M., Baker, A., Larson, T. R. and Graham, I. A. (2005) *Plant Physiol.* **137**, 835-840
7. Hu, J. P., Aguirre, M., Peto, C., Alonso, J., Ecker, J. and Chory, J. (2002) *Science* **297**, 405-409
8. Schumann, U., Wanner, G., Veenhuis, M., Schmid, M. and Gietl, C. (2003) *Proc. Natl. Acad. Sci. U. S. A.* **100**, 9626-9631
9. Sparkes, I. A., Brandizzi, F., Slocombe, S. P., El-Shami, M., Hawes, C. and Baker, A. (2003) *Plant Physiol.* **133**, 1809-1819
10. Footitt, S., Slocombe, S. P., Larner, V., Kurup, S., Wu, Y., Larson, T. R., Graham, I. A., Baker, A. and Holdsworth, M. (2002) *Embo J.* **21**, 2912-2922
11. Hettema, E. H., Girzalsky, W., van den Berg, M., Erdmann, R. and Distel, B. (2000) *Embo J.* **19**, 223-233
12. South, S. T., Sacksteder, K. A., Li, X. L., Liu, Y. F. and Gould, S. J. (2000) *J. Cell Biol.* **149**, 1345-1359
13. South, S. T. and Gould, S. J. (1999) *J. Cell Biol.* **144**, 255-266
14. Honsho, M., Hiroshige, T. and Fujiki, Y. (2002) *J. Biol. Chem.* **277**, 44513-44524
15. Gotte, K., Girzalsky, W., Linkert, M., Baumgart, E., Kammerer, S., Kunau, W. H. and Erdmann, R. (1998) *Mol. Cell. Biol.* **18**, 616-628
16. Matsuzono, Y., Kinoshita, N., Tamura, S., Shimozawa, N., Hamasaki, M., Ghaed, K., Wanders, R. J. A., Suzuki, Y., Kondo, N. and Fujiki, Y. (1999) *Proc. Natl. Acad. Sci. U. S. A.* **96**, 2116-2121

17. Snyder, W. B., Faber, K. N., Wenzel, T. J., Koller, A., Luers, G. H., Rangell, L., Keller, G. A. and Subramani, S. (1999) *Mol. Biol. Cell* **10**, 1745-1761
18. Soukupova, M., Sprenger, C., Gorgas, K., Kunau, W. H. and Dodt, G. (1999) *Eur. J. Cell Biol.* **78**, 357-374
19. Hoepfner, D., Schildknegt, D., Braakman, I., Philippsen, P. and Tabak, H. F. (2005) *Cell* **122**, 85-95
20. Ghaedi, K., Tamura, S., Okumoto, K., Matsuzono, Y. and Fujiki, Y. (2000) *Mol. Biol. Cell* **11**, 2085-2102
21. Sacksteder, K. A., Jones, J. M., South, S. T., Li, X. L., Liu, Y. F. and Gould, S. J. (2000) *Journal of Cell Biology* **148**, 931-944
22. Snyder, W. B., Koller, A., Choy, A. J. and Subramani, S. (2000) *J. Cell Biol.* **149**, 1171-1177
23. Lambkin, G. R. and Rachubinski, R. A. (2001) *Mol. Biol. Cell* **12**, 3353-3364
24. Otzen, M., Perband, U., Wang, D., Baerends, R. J. S., Kunau, W. H., Veenhuis, M. and Van der Klei, I. J. (2004) *J. Biol. Chem.* **279**, 19181-19190
25. Jones, J. M., Morrell, J. C. and Gould, S. J. (2004) *J. Cell Biol.* **164**, 57-67
26. Fransen, M., Vastiau, I., Brees, C., Brys, V., Mannaerts, G. P. and Van Veldhoven, P. P. (2004) *J. Biol. Chem.* **279**, 12615-12624
27. Fransen, M., Wylin, T., Brees, C., Mannaerts, G. P. and Van Veldhoven, P. P. (2001) *Mol. Cell. Biol.* **21**, 4413-4424
28. Rottensteiner, H., Kramer, A., Lorenzen, S., Stein, K., Christiane, L. F., Volkmer-Engert, R. and Erdmann, R. (2004) *Mol. Biol. Cell* **15**, 3406-3417
29. Fang, Y., Morrell, J. C., Jones, J. M. and Gould, S. J. (2004) *J. Cell Biol.* **164**, 863-875
30. Fransen, M., Vastiau, I., Brees, C., Brys, V., Mannaerts, G. P. and Van Veldhoven, P. P. (2005) *J. Mol. Biol.* **346**, 1275-1286
31. Shibata, H., Kashiwayama, Y., Imanaka, T. and Kato, H. (2004) *J. Biol. Chem.* **279**, 38486-38494
32. Mayerhofer, P. U., Kattenfeld, T., Roscher, A. A. and Muntau, A. C. (2002) *Biochem. Biophys. Res. Commun.* **291**, 1180-1186
33. Sambrook, J. and Russell, D. W. (2001) Molecular cloning, a laboratory manual.3rd Ed., Cold Spring Harbour Laboratory Press, New York
34. Tugal, H. B., Pool, M. and Baker, A. (1999) *Plant Physiol.* **120**, 309-320
35. Lopez-Huertas, E., Sandalio, L. M. and Delrio, L. A. (1995) *Plant Physiol. Biochem.* **33**, 295-302
36. Combet, C., Blanchet, C., Geourjon, C. and Deleage, G. (2000) *Trends Biochem.Sci.* **25**, 147-150
37. Zimmermann, P., Hirsch-Hoffmann, M., Hennig, L. and Gruissem, W. (2004) *Plant Physiol.* **136**, 2621-2632
38. Boyes, D. C., Zayed, A. M., Ascenzi, R., McCaskill, A. J., Hoffman, N. E., Davis, K. R. and Gorlach, J. (2001) *Plant Cell* **13**, 1499-1510
39. Sagne, C., Isambert, M. F., Henry, J. P. and Gasnier, B. (1996) *Biochem. J.* **316**, 825-831
40. Zacharias, D. A., Violin, J. D., Newton, A. C. and Tsien, R. Y. (2002) *Science* **296**, 913-916
41. Abe, Y., Shodai, T., Muto, T., Mihara, K., Torii, H., Nishikawa, S.-i., Endo, T. and Kohda, D. (2000) *Cell* **100**, 551-560
42. Brix, J., Rudiger, S., Bukau, B., Schneider-Mergener, J. and Pfanner, N. (1999) *J. Biol. Chem.* **274**, 16522-16530
43. Notredame, C., Higgins, D. G. and Heringa, J. (2000) J. Mol. Biol. 302, 205-217

FOOTNOTES

Acknowledgements-
We thank Dr Thierry Desprez, INRA, Versailles for the EST clone ATTS4952 and Susanna Cristobal, University of Uppsala, Sweden for the His_6PEX19 expression clone, Alison Ashcroft, Mass spectrometry Facility, Faculty of Biological sciences, University of Leeds for MALDI-MS, James Williams for constructing His_6T7PEX19, Barbara Johnson for excellent technical assistance and the Biotechnology and Biological Sciences Research Council (BBSRC) for financial support.

The abbreviations used are:
PMP, peroxisomal membrane protein; mPTS, region containing peroxisome targeting information; TMD, transmembrane domain; PBS, phosphate buffered saline; GST, glutathione s-transferase; SDS, sodium dodecyl sulfate; CD, circular dichroism; MALDI-MS, matrix assisted laser desorption/ionisation mass spectrometry.

FIGURE LEGENDS

Fig. 1**.** *Arabidopsis* contains two homologues of HsPEX19. Alignment of *Arabidopsis PEX19-1* and *19-2* with human *PEX19* and *Saccharomyces cerevisiae PEX19*. Amino acid sequences were aligned with the programme T-COFFEE [43]. Grey shading indicates hydrophobic residues in conserved regions that are predicted to form amphipathic helices. The CAAX motif directing farnesylation is indicated in bold. The cleavage site for trypsin in human *PEX19* is indicated by an arrow.

Fig. 2. Expression profiles of *Arabidopsis PEX19-1*. Expression profiles were constructed from public microarray data using tools available on the GENEVESTIGATOR website [37]. *A*, Expression in various plant organs generated by the Gene Atlas tool. *B*, Expression at different developmental stages, defined by [38]. Stage 0, seed germination; stage 1, leaf development; stage 3, rosette growth; stage 5, inflorescence emergence; stage 6, flower production; stage 8, silique development generated by the gene chronologer tool.

Fig. 3. *Arabidopsis* PEX19 is predominantly a cytosolic protein. *A*, Anti-PEX19 antibodies recognise native PEX19, a 30 kDa protein in *Arabidopsis* seedlings. Left panel, immunoblot probed with anti-PEX19 anti-serum 1:10,000 dilution; lane 1, 10 ng recombinant His_6T7PEX19, lane 2, 1 ng His_6T7PEX19, lane 3, total protein extract equivalent to twenty 2 day old *Arabidopsis* seedlings. Right panel, as for left panel except that the anti-PEX19 antiserum was preincubated with 10 μg His_6T7PEX19 prior to immunodecoration of the blot. *B*. PEX19 is mainly cytosolic. Tissue culture cells were separated into a cytosolic fraction (100,000 x g supernatant), lane 1 and a membrane associated fraction (100,000 x g pellet), lane 2 and probed with anti-PEX19 serum. *C*. An organelle fraction prepared from tissue culture cells was separated by sucrose density gradient centrifugation and the fractions blotted and detected with anti-thiolase (top panel) and anti-PEX19 (lower panel). The star indicates a recombinant His_6T7PEX19 standard in lane 1. The arrow indicates the native PEX19.

Fig. 4. Recombinant His_6PEX19 forms a dimer**.** *A*, rHis_6PEX19 (previously purified by nickel affinity chromatography, data not shown) was applied to a gel filtration column and eluted with a retention volume of 115 ml (shown by downward pointing arrow) indicating it has a mass of 60 kDa, consistent

with a dimer. The column was calibrated using a gel filtration low molecular weight calibration kit (GE Health Care) with retention volumes and masses of the protein standards indicated on the chromatogram (upward pointing arrows). V_0 is the void volume. *B*, Coomassie stained SDS-PAGE of $rHis_6PEX19$ in fractions eluted from the gel filtration column. His_6PEX19 in fractions between 110 and 135 ml (indicated by hatched double arrows on *A* and *B*) show that it migrates with an apparent mass of approximately 30 kDa in SDS-PAGE, despite elution from the column with a mass of approximately 60 kDa. The lane indicated as *P* shows $rHis_6PEX19$ before gel filtration chromatography.

Fig. 5. *In vitro* translated AtPEX19-1 interacts with PEX10. His_6PEX19-1 and PEX10 were in vitro translated and mixed (lane B) prior to immunoprecipitation by non-immune serum (PI) or anti-His antibodies (H) followed by SDS-PAGE and phosphoimaging. Solid arrow indicates the position of PEX19-1, open arrow indicates the position of PEX10. ^{14}C Molecular weight standards are indicated.

Fig. 6. Recombinant His_6PEX19 binds to the C-terminus of PEX10. Pull down experiments using lysates from *E. coli* expressing His_6PEX19 (*PEX19*) or GST-$PEX10_{267-381}$ (*PEX10*) were performed; The lysates were applied alone or as a mixture of both, to a glutathione column, the flow through collected, column washed and specifically bound material was eluted with 10 mM reduced glutathione. The fractions (*P*, sample prior to column application, *FT*, flow through, *W*, wash and *E*, eluate) were analysed by Western blot, immuno-stained with anti-PEX19 (*panel A*) or anti-GST (*panel B*) antibodies. Positions of His_6PEX19 (*panel A*) and GST-$PEX10_{267-381}$ (*panel B*) are indicated by arrows

Fig. 7. The dimeric form of PEX19 is preferentially cross-linked to other proteins *in vivo*. *Arabidopsis* suspension cells were cross-linked *in vivo* with 1% formaldehyde. *A*, The cell lysates, cross-linked, (lane +) or not cross-linked (lane -), were examined by immunoblotting using antiserum raised against recombinant His_6PEX19 at 1:10,000 dilution. *B*, As panel A, but the antisera was incubated with $rHis_6PEX19$ (10 μg) for 30 minutes at 37ºC before immunodecoration of the blot.

Fig. 8. The possible interactions of PEX19 and PEX3 in the targeting and insertion of PMPs. *A*, Clustal W alignment of PEX3 sequences from *Arabidopsis*, human and *S. cerevisiae*. Underlined, predicted binding sites for ScPex19p, italics, experimentally determined binding site for HsPEX19. *B*, Model showing the possible roles of the two PEX19 binding sites (BS) of PEX3 and the two PEX3 binding sites on PEX19 in the targeting and insertion of PMPs (shown in orange). The interaction between the N-terminal PEX3 binding site on PEX19 and the second PEX19 binding site on PEX3 provides the docking interaction. We propose that the function of the second PEX19 binding site on PEX3 is to displace the mPTS in the vicinity of the membrane. Membrane insertion may then be spontaneous, catalysed by PEX3 or another unknown factor (not shown).


AtPEX19-1 --------MAN-S--HTDDLDELLDSALDDFKDLNLSHQRNQREAQEEEEKKRKEETVLL
AtPEX19-2 --------MANDT--HTDDLDELLDSALDDFKDLNLT----QRNGGVKKEEGDKKETESL
HsPEX19 MAAAEEGCSVGAE--ADRELEELLESALDDFDKAKPSPAPPSTTTAPDASGPQKRSPGDT
ScPEX19 MPNIQHEVMNENEYDNFDDLDDLLDEDPTKLDEAEPDDVQAKGSVYNDSENKEKNAESKD
AtPEX19-1 PSGVQ----------
AtPEX19-2 PSGVQ----------
HsPEX19 AKDALFASQEKFFQELF----------
ScPEX19 SDGVQVANESEEDPELKEMMVDLQNEFANLMKNNGNENNVKTEDFNKLISALEEAAKVPH
AtPEX19-1 -GLGMGLPDMRSKKRGKQKVSKEDH-----VAEALDKLREQT----------R
AtPEX19-2 -GLGMGLPDMRSKKKGKKKIAKEDH-----VTEALDKLREQT----------R
HsPEX19 DSELASQATAEFEKAMKELAEEEPH-----LVEQFQKLSEAAGRVGSDMTSQQEFTSCLK
ScPEX19 QQMEQGCSSLKSNSTDKGTVNGSNPGFKNIVSNTLDRLKENG----------N
AtPEX19-1 ETVKGLESISSKQLPASDDDGMVEDFLKQFED----------L-----AGSKDLESIVET
AtPEX19-2 ETVKGLESLSSKQQPTGSDDAMVEDWIKQFEN----------L-----TGSNDLESIVDT
HsPEX19 ETLSGLAKNATDLQNSSMSE---EELTKAMEG----------LGMDEGDGEGNILPIMQS
ScPEX19 KVDTSLAEETKESQRSGQN-NNIDDILSQLLDQMVASGGKESAENQFDLKDGEMDDAITK
AtPEX19-1 MMQQLLSKDILHEPMKELGARYPKWLKEN-EASLSKEDYKRYSQQYKLIEELNAVYE---
AtPEX19-2 MMQQLLSKDILHEPMKEIGARYPKWLEEH-ESSLNKEEFDRYSRQYELIKELNLVYE---
HsPEX19 IMQNLLSKDVLYPSLKEITEKYPEWLQSH-RESLPPEQFEKYQEQHSVMCKICEQFE---
ScPEX19 ILDQMTSKEVLYEPMKEMRSEFGVWFQENGENEEHKEKIGTYKRQFNIVDEIVNIYELKD
AtPEX19-1 -NEPNNSSK---------IMEIMQKMQECGQPP----------SDIVKEIDPGFDF
AtPEX19-2 -NEPNNSTK---------IMEIMQKMQECGQPP----------SDIVQEMDPGFDF
HsPEX19 -AETPTDSETTQKARFEMVLDLMQQLQDLGHPP----------KELAGEMPPGLNF
ScPEX19 YDELKHKDR---------VTELLDELEQLGDSPIRSANSPLKHGNEEEELMKMLEIDGND
AtPEX19-1 -ASLGQISPEMLESSPNCCIM
AtPEX19-2 -ASLGQMSPDMLESSPNCCVM
HsPEX19 DLDALNLSGPPGASGEQCLIM
ScPEX19 -PNLGNLDKELTDGCKQQ---

Figure 1

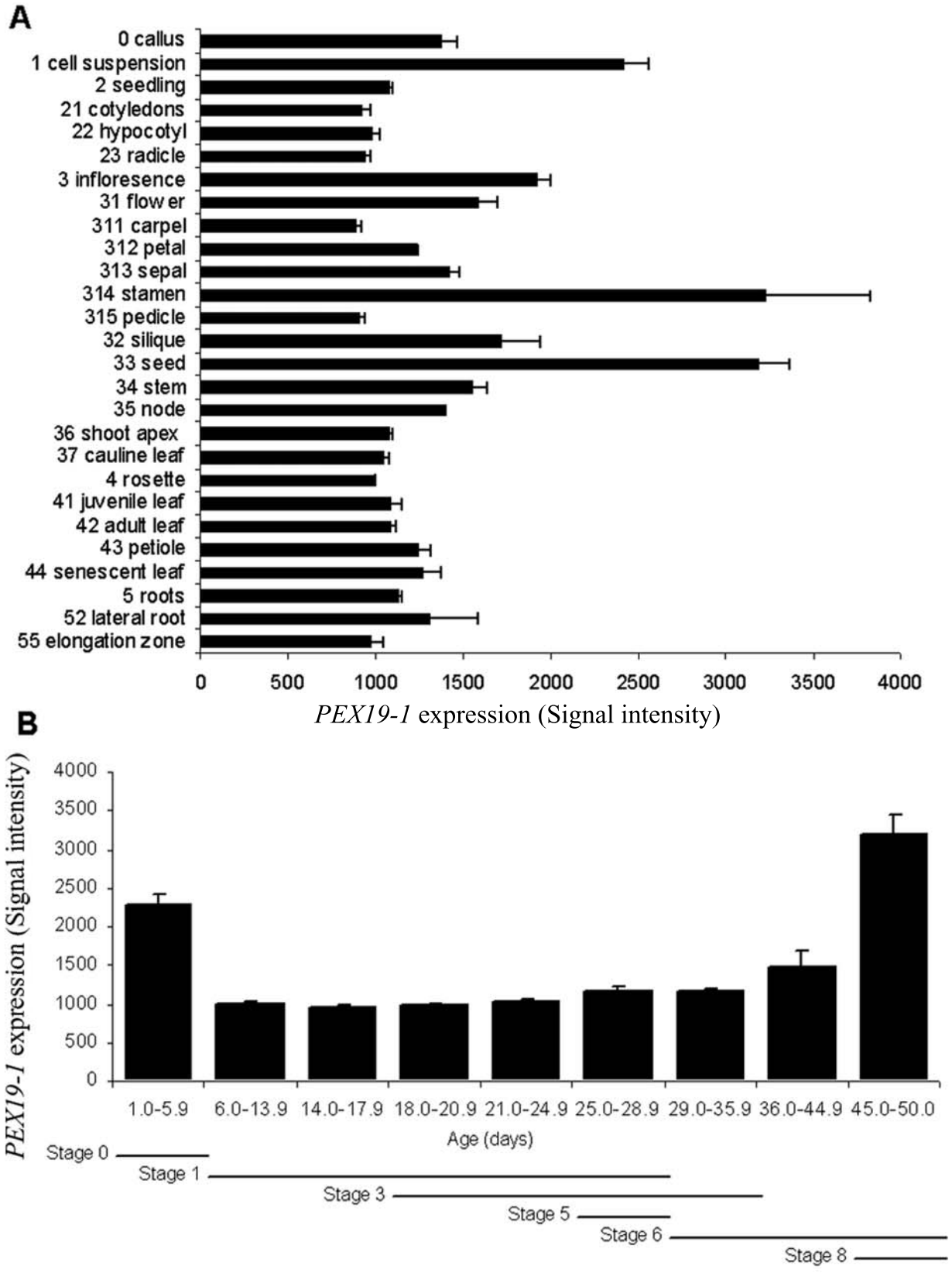
A
0 callus
1 cell suspension
2 seedling
21 cotyledons
22 hypocotyl
23 radicle
3 infloresence
31 flower
311 carpel
312 petal
313 sepal
314 stamen
315 pedicle
32 silique
33 seed
34 stem
35 node
36 shoot apex
37 cauline leaf
4 rosette
41 juvenile leaf
42 adult leaf
43 petiole
44 senescent leaf
5 roots
52 lateral root
55 elongation zone
0
500
1000
1500
2000
2500
3000
3500
4000
PEX19-1 expression (Signal intensity)
B
PEX19-1 expression (Signal intensity)
4000
3500
3000
2500
2000
1500
1000
500
0
1.0-5.9
6.0-13.9
14.0-17.9
18.0-20.9
21.0-24.9
25.0-28.9
29.0-35.9
36.0-44.9
45.0-50.0
Age (days)
Stage 0
Stage 1
Stage 3
Stage 5
Stage 6
Stage 8

Figure 2

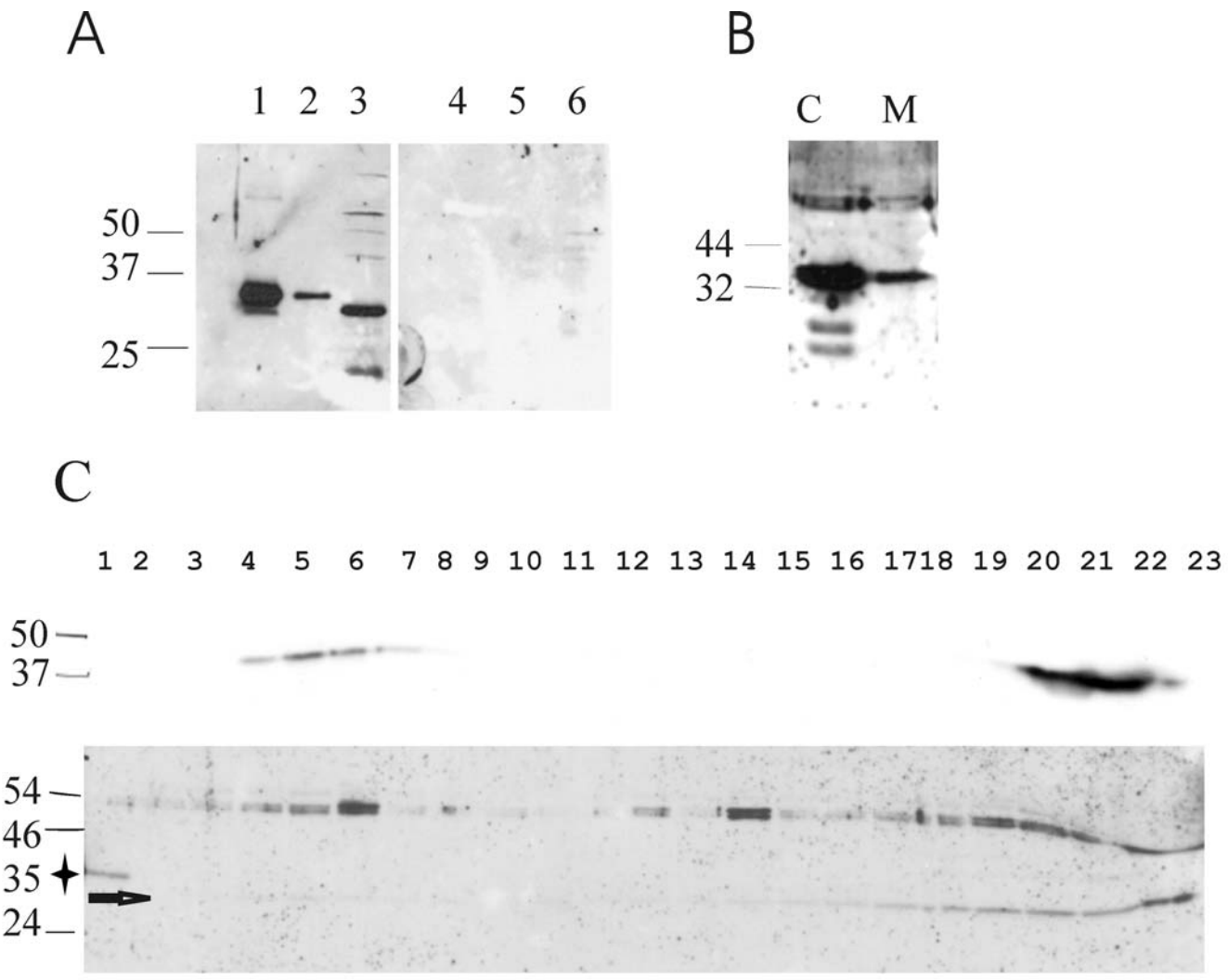
A
1 2 3 4 5 6
50
37
25
B
C M
44
32
C
1 2 3 4 5 6 7 8 9 10 11 12 13 14 15 16 17 18 19 20 21 22 23
50
37
54
46
35
24

Figure 3

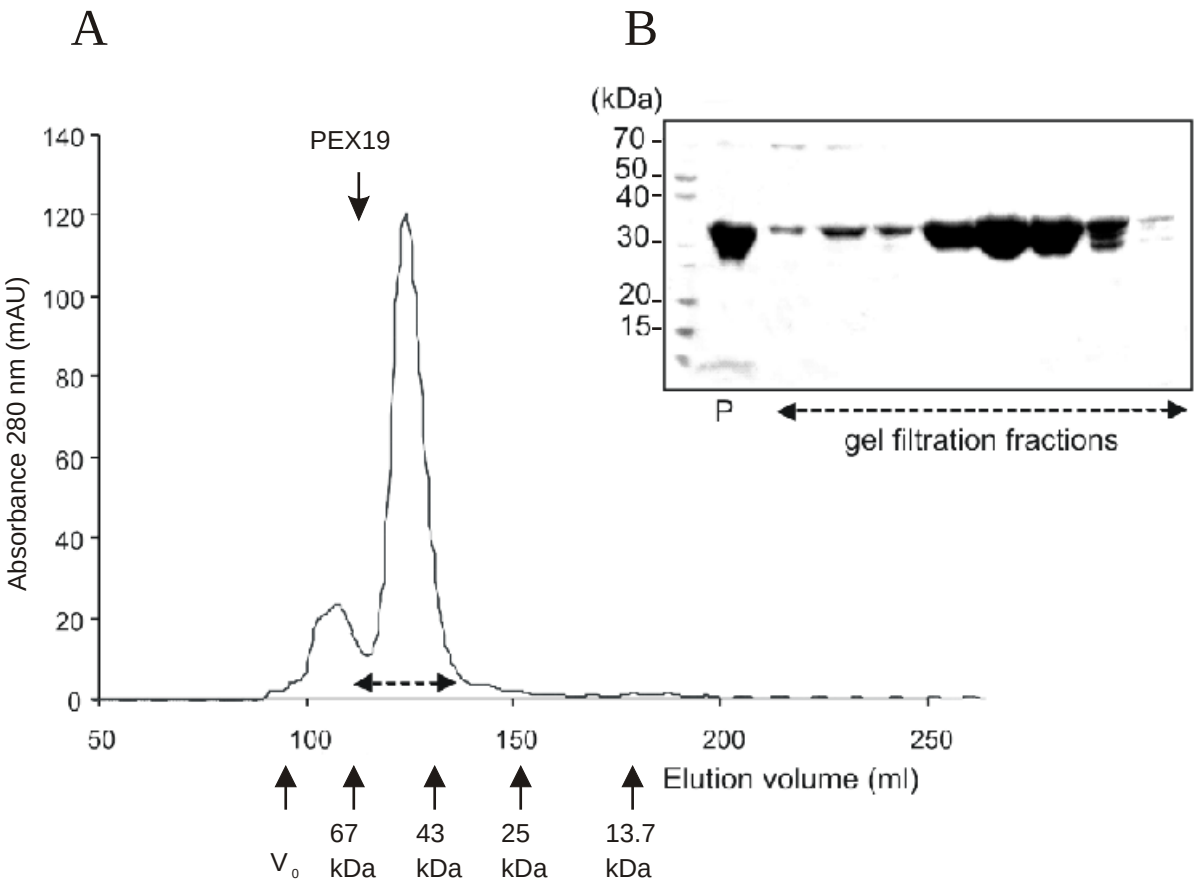
A
B
(kDa)
70
50
40
30
20
15
P
gel filtration fractions
PEX19
Absorbance 280 nm (mAU)
140
120
100
80
60
40
20
0
50
100
150
200
250
Elution volume (ml)
V0
67 kDa
43 kDa
25 kDa
13.7 kDa

Figure 4

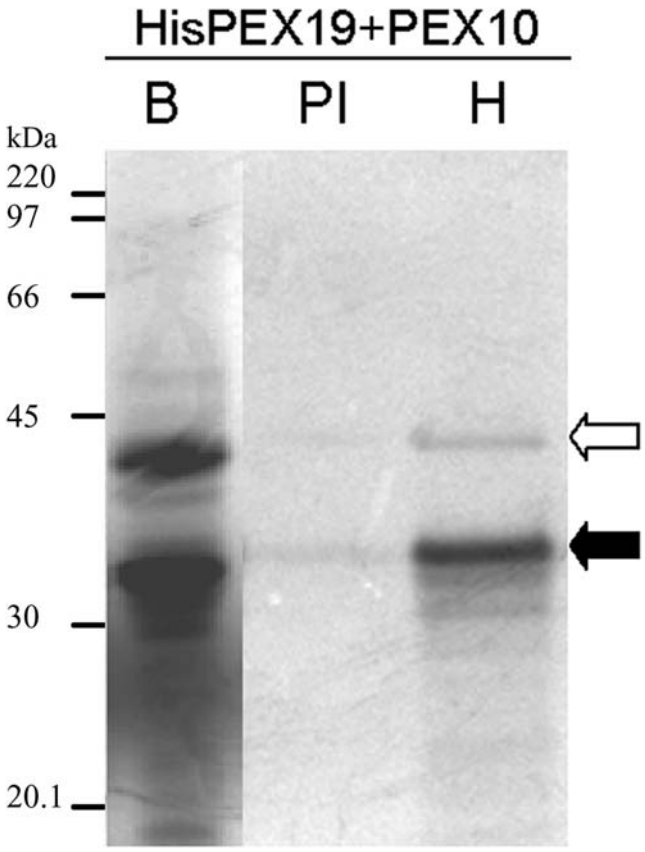

Figure 5

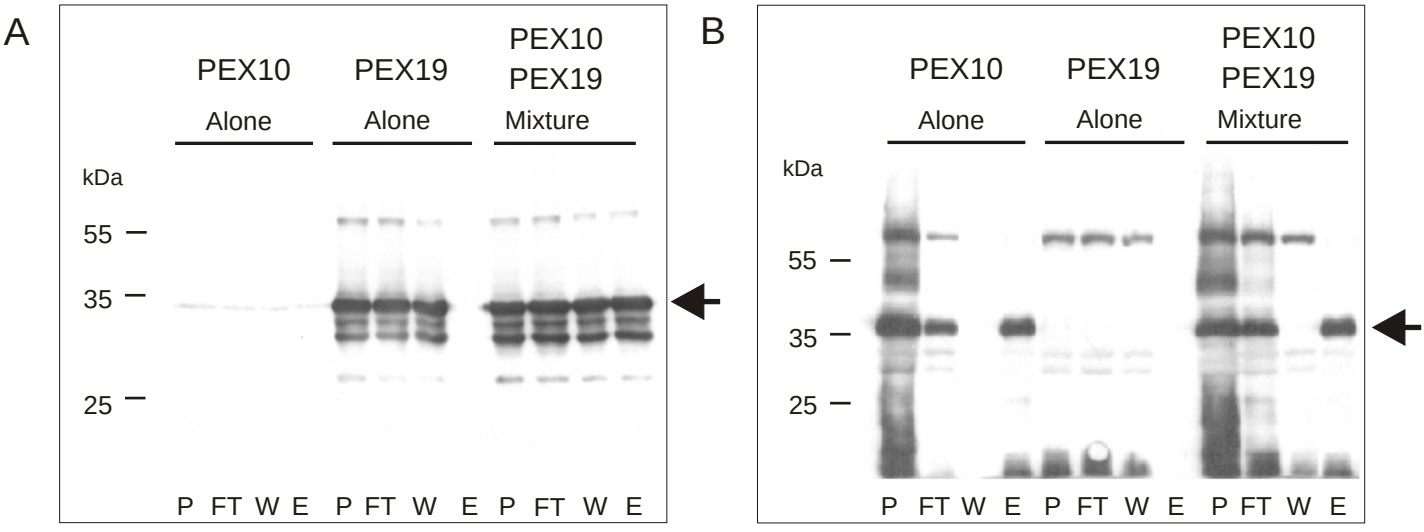
A
PEX10
PEX19
PEX10
PEX19
Alone
Alone
Mixture
kDa
55
35
25
P FT W E P FT W E P FT W E
B
PEX10
PEX19
PEX10
PEX19
Alone
Alone
Mixture
kDa
55
35
25
P FT W E P FT W E P FT W E

Figure 6

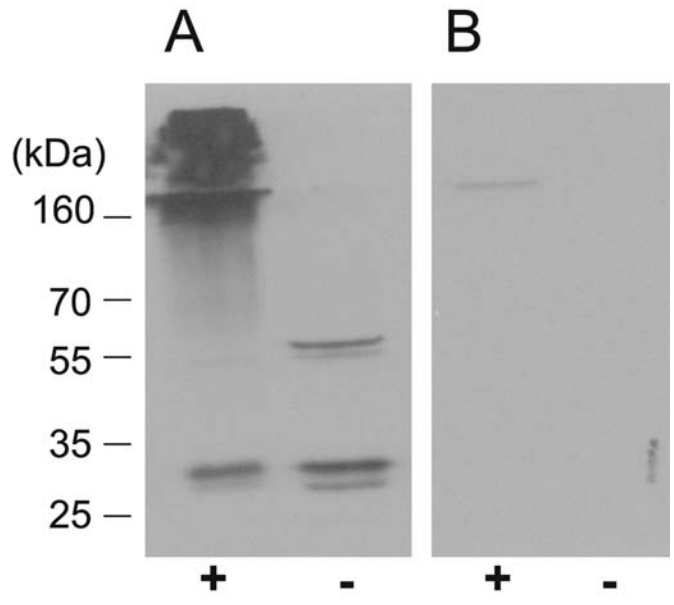

Figure 7

A

```
AtPEX3          ---MDFVRGFWRKHRRKVLVTAGCLGSGYLLYK----LYNSHTRRLADLERELAHEREND
HsPEX3          --MLRSVWNFLKRHKKKCIFLGTVLGGVYILGK----YGQKKIREIQ--EREAA-----E
ScPEX3          MAPNQRSRSLLQRHRGKVLISLTGIAALFTTGSVVVFFVKRWLYKQQ--LRITE-----Q
                        .: ::*: * :.    :.. :   .      :    .     *       :
AtPEX3          EIIKTQMKAHFESIQMIVDSTTLPHAMQFLSIRISEE-IDVSHVMDRLNQG---------
HsPEX3          YIAQARRQYHFESNQRTCNMTVLSM-LPTLREALMQQ-LN-SESLTALLKN---------
ScPEX3          HFIKEQIKRRFEQTQEDSLYTIYEL-LPVWRMVLNENDLN-LDSIVTQLKDQKNQLTRAK
                 : : : : :**. *     *     :      : :: ::  . :    :.
AtPEX3          --KGMLSPP--EKLQLWDELKILSFTRMVLSLWSVTMLSLYIRVQVNILGRHLYVDTARA
HsPEX3          --R----PS--NKLEIWEDLKIISFTRSTVAVYSTCMLVVLLRVQLNIIGGYIYLDNAAV
ScPEX3          SSESRESSPLKSKAELWNELELKSLIKLVTVTYTVSSLILLTRLQLNILTRNEYLDSAIK
                  .    ..  .* ::*::*:: *: : .   ::.  * :  *:*:**:    *:*.*
```

B

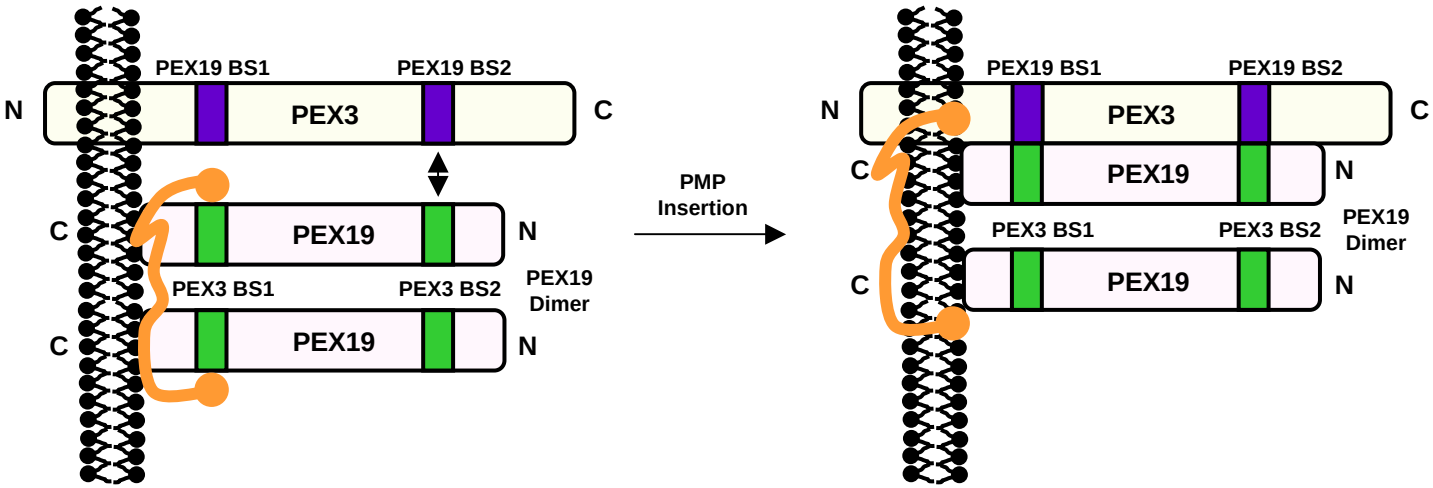

Figure 8